Influence of Manufacturing Errors on the Dynamic Characteristics of Planetary Gear Systems

Gill-Jeong Cheon*
Division of Mechanical Engineering, Wonkwang University, Iksan City, Jeon-Buk, 570-749, Korea
Robert G. Parker
Department fo Mechanical Engineering, The Ohio State University, Columbus, OH 43220-1107, USA

A dynamic analysis using a hybrid finite element method was performed to characterize the effects of a number of manufacturing errors on bearing forces and critical tooth stress in the elements of a planetary gear system. Some tolerance control guidelines for managing bearing forces and critical stress are deduced from the results. The carrier indexing error for the planet assembly and planet runout error are the most critical factors in reducing the planet bearing force and maximizing load sharing, as well as in reducing the critical stress.

Key Words : Planetary Gear, Manufacturing Error, Thickness Error, Runout Error, Position Error

1. Introduction

A planetary gear system composed of multiple gear components has a more complicated geometry than conventional parallel shaft gear systems. The behavior of the whole system is affected by errors in the shape or position of individual elements. Some manufacturing errors, such as errors in gear runout, tooth thickness, or the positioning of the planet carrier mounting holes, are unavoidable in real systems.

Although these factors are important when defining tolerances at the design stage, studies of the effects of these types of error are scarce. Bodas and Kahraman (2001) analyzed the effects of manufacturing errors on the static planet load sharing behavior. They focused on the effects on planet load sharing of errors in the position, runout, and tooth-thickness of planet gears. James and Harris (2002) analyzed the effect of the radial internal clearance of the planet bearing and planet pin position error on unequal planet load sharing. However, they restricted their analysis to planet load sharing caused by planet related errors. The main causes of planetary gear system failure are failures of the gears and bearings (Townsend, 1991), which are directly related to critical (maximum) tooth stress and bearing reaction forces.

The purpose of this work was to characterize the effects of various errors on the dynamic properties of a planetary gear system. Errors in the sun, ring, and planet gears were included in an analysis of the effects on bearing forces, critical tooth stress, and load sharing. Tooth thickness, runout, and position errors were considered in this study, as these are the most common gear system manufacturing errors related to tolerance control. The types of errors that most affect the bearing force, critical tooth stress, and load sharing were determined.

* Corresponding Author,
E-mail : gjcheon@wonkwang.ac.kr
TEL : +82-63-850-6686; **FAX** : +82-63-850-6691
Division of Mechanical Engineering, Wonkwang University, Iksan City, Jeon-Buk, 570-749, Korea. (Manuscript **Received** August 12, 2003; **Revised** January 5, 2004)

2. Computational Model

The nominal rigid body motions of the components were determined using basic planetary gear kinematics (Cheon et al., 1999; Kahraman, 1994; Lin and Parker, 1999; Youn and Cheon, 2003). The computational model calculated gear component deflections relative to the nominal motions (static transmission error), as well as elastic tooth deflections/stresses and bearing loads. A hybrid finite element method was used to compute two dimensional deformations and the stresses on gear components. To avoid generating an extremely large number of elements to model the continuously moving contact zones, they were divided into two separate regions. For the contact region closest to the tooth surface (inner region), the Bousinesq solution for a point load acting on a half-space and contact forces are integrated over the tooth contact region to accurately represent relative displacements, though absolute displacements will not be accurate because of overall tooth bending about the root. Outside the immediate vicinity of the contact zone (outer region), finite element analysis effectively models the elastic body response, including gross deflections associated with tooth bending. The two solutions were matched along the interface between the inner and outer regions. The constraints imposed by the contact between mating surfaces are essentially linear inequality constraints. A Revised simplex algorithm is used to efficiently solve the unknown loads within a number of iterations. Attaching a reference frame to each individual component separately, a search was carried out over all possible surface pairings to determine which surface instances could make contact. The changing mesh stiffness and contact forces were evaluated internally at each time step as the gears rolled through the mesh. Details can be found in the references (ANSol, 2003; Kahraman and Vijayakar, 2001; Parker et al., 2000b; Vijayakar, 1991).

In a planetary gear system, each gear undergoes large rotation according to kinematic relationships. The elastic deformations of the gears that superpose on the rigid body motion are small. By measuring the finite element displacement vector $\mathbf{X}_{fi}$ for a particular gear i with respect to a reference frame that follows the rigid body motion, it is possible to represent its behavior by a linear system of differential equations (Parker et al., 2000b)

$$\mathbf{M}_{ffi}\ddot{\mathbf{X}}_{fi}+\mathbf{C}_{ffi}\dot{\mathbf{X}}_{fi}+\mathbf{K}_{ffi}\mathbf{X}_{fi}=\mathbf{f}_{fi} \tag{1}$$

where $\mathbf{f}_{fi}$ is the vector of specified external loads. Rayleigh's damping model is used in the form

$$\mathbf{C}_{ffi}=\mu\mathbf{M}_{ffi}+\eta\mathbf{K}_{ffi} \tag{2}$$

μ and η are constant Rayleigh coefficients, and are adjusted to satisfy damping properties of the material. In this study, 479 and 1.2×10^{-7} are used for μ and η, respectively. Representing the rigid body motions of the reference frame by $\mathbf{X}_{ri}$ and combining it with equation (1) results in

$$\begin{bmatrix}\mathbf{M}_{ffi} & \mathbf{M}_{fri}\\ \mathbf{M}_{rfi} & \mathbf{M}_{rri}\end{bmatrix}\begin{Bmatrix}\ddot{\mathbf{X}}_{fi}\\ \ddot{\mathbf{X}}_{ri}\end{Bmatrix}+\begin{bmatrix}\mathbf{C}_{ffi} & \mathbf{C}_{fri}\\ \mathbf{C}_{rfi} & \mathbf{C}_{rri}\end{bmatrix}\begin{Bmatrix}\dot{\mathbf{X}}_{fi}\\ \dot{\mathbf{X}}_{ri}\end{Bmatrix}+\begin{bmatrix}\mathbf{K}_{ffi} & \mathbf{K}_{fri}\\ \mathbf{K}_{rfi} & \mathbf{K}_{rri}\end{bmatrix}\begin{Bmatrix}\mathbf{X}_{fi}\\ \mathbf{X}_{ri}\end{Bmatrix}=\begin{Bmatrix}\mathbf{f}_{fi}\\ \mathbf{f}_{ri}\end{Bmatrix} \tag{3}$$

The equations for each gear are assembled into the entire planetary gear system as

$$\mathbf{M}\ddot{\mathbf{X}}+\mathbf{C}\dot{\mathbf{X}}+\mathbf{K}\mathbf{X}=\mathbf{f} \tag{4}$$

$\mathbf{M}$, $\mathbf{C}$ and $\mathbf{K}$ represent mass, damping and stiffness matrices for the system. The Newmark method was used for time integration of the equation of motion.

The system analyzed was the Army OH-58 Kiowa helicopter planetary gear. Figure 1 shows the schematics of this system, which has four

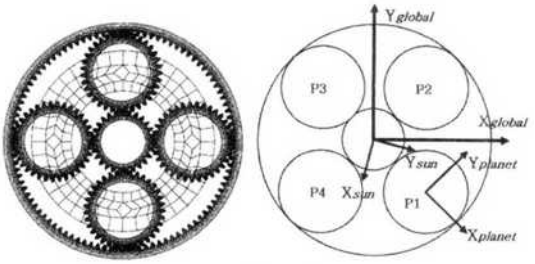

Fig. 1 Schematics of a four planet gear system; the input sun gear rotates clockwise

planets, and the parameters are given in Table 1. The operating pressure angles between sun-planet and planet-ring are 24.6° and 20.19°, respectively. This is a spur gear system so a two dimensional model was adopted. The outer ring gear circle was rigidly fixed with no deformation, although tooth deflection was allowed. The inner races of the sun and planets were modeled as rigid circles supported by isotropic, linear bearings. The bearings were modeled as rigid outer and inner races connected by a 3×3 diagonal stiffness matrix containing elements of magnitude 87.6×10^6 N/m for the two dimensional translational degrees of freedom. The stiffness for rotational motion was zero. The elastically deformable teeth were modeled as spurs with perfect involute shape. Two different systems having either three or four planet gears were examined; gear elements are identical in both configurations. While the planets were equally spaced with same mesh phasing for the three planet case, the planets in the four planet case were unequally spaced with different mesh phasing at 0°, 91.4°, 180°, and 271.4°. A constant external sun gear input torque comprised the external forcing. The nominal input speed and torque were 1620 rpm and 1412 N-m, respectively. The output shaft was connected to the carrier, whose rotational deflection was constrained to zero. The time step was 0.0001 sec, and the number of time steps per one mesh cycle was 27.

Table 1 Gear data for the OH-58 Kiowa planetary gear set

	Sun	Ring	Planet
Number of Teeth	27	99	35
Module (mm)	2.868	2.778	2.868
Outer Diameter (mm)	84.07	304.8	105.0
Root Diameter (mm)	70.55	284.1	91.54
Minor Diameter (mm)		271.8	
Bore Diameter (mm)	57.15		73.66
Face Width (mm)	25.4		
Young's Modulus (N/m^2)	207×10^9		
Poisson's Ratio	0.3		
Density (Kg/m^3)	7595		

The sun, carrier, and planet bearing forces were calculated to be absolute resultant forces without regard to the directional variation. Both of tensile and compressive maximum principal stresses over the root/fillet region were calculated. Because sun gear was smaller than planet in our model, sun gear teeth engaged much more frequently than planet and ring gear teeth, and the maximum stresses of sun gear was always larger than those of other gears. Hence, only the maximum absolute values of the maximum and minimum principal normal stresses of sun gear were traced as the maximum and minimum critical stresses.

The sun, carrier, and ring gear were nominally central, coaxial elements. The axis of the carrier was assumed to be the origin for the fixed reference frame. Ideally, the sun and ring gear axes align with this origin. However, an assembly error can cause the centers of the sun and ring to be non-coincident with that of the carrier. Alternatively, the position of the holes machined on the carrier for the planet pin or bearing can be slightly displaced from the ideal position. In this study, positioning errors of the sun and ring gears were specified only in the positive x direction of the global coordinates. Only one of the planets (Planet 1) was assumed to have a positioning error, and the error was specified as in the radial or tangential direction (Fig. 1).

Runout error can be generated by making the axis of a gear non-coincident with the center of its pitch circle. In case of planet, only one of the planets (Planet 1) was assumed to have runout error, and the error was specified in the x direction of the planet's coordinates.

The thickness error is the amount by which the circular tooth thickness at the pitch circle is more than the nominal amount. The thickness error is applied to the tooth by rotating the contact surfaces about the pitch circle center. When whole teeth of the sun or ring gear were supposed to have thickness errors, magnitudes and patterns of the bearing forces were almost similar to those of normal condition irrespective of the error size. Because sun and ring gear mesh with four planets simultaneously, the effects of thickness error cancelled each other by symmetric meshing. Hence,

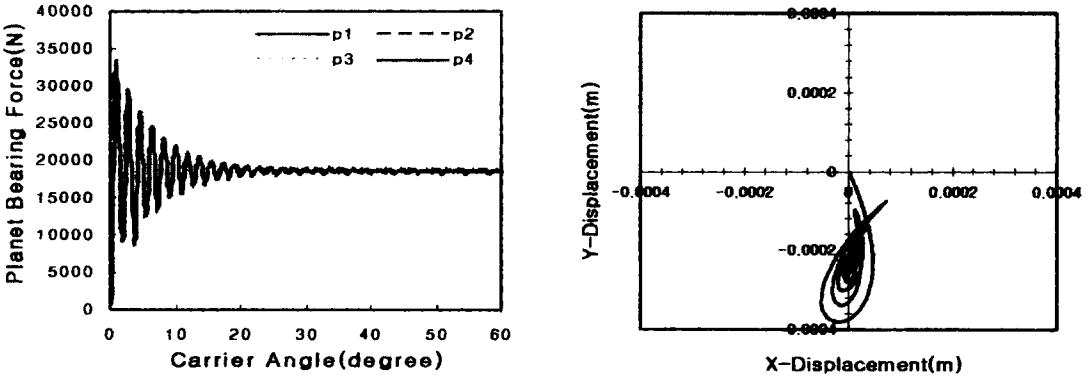

Fig. 2 Planet bearing forces and the loci of one planet center under normal conditions with four planets

only successive one fourth of sun and ring gear teeth were supposed to have thickness errors to guarantee at least one tooth with error keeps on asymmetric meshing with one of four planets. And all the teeth of one planet (Planet 1) were supposed to have a thickness error.

Loads on each planet bearing F_i were compared by the load sharing (LS) of each planet as

$$LS_i=\frac{F_i}{\sum_{j=1}^{N}F_j},\ \text{i=1 to N (N=3 or 4)} \qquad (5)$$

where N is the total number of planets in the gear set. Overload sharing is defined as the peak value of the load sharing over the mean average value (25% in four planets, 33.3% in three planets).

According to Bodas and Kahraman (2001), the load sharing is proportional to the absolute magnitude of the error. Hence, the size of the error was selected as positive 25 μm and 50 μm for the four planet case and 25 μm for the three planet case.

All the positioning, runout, and thickness errors were assigned to be positive in this analysis.

3. Parametric Studies

3.1 Normal conditions

Figure 2 shows the planet bearing forces and the loci of one planet center ($p1$) under normal conditions with four planets. The system arrives

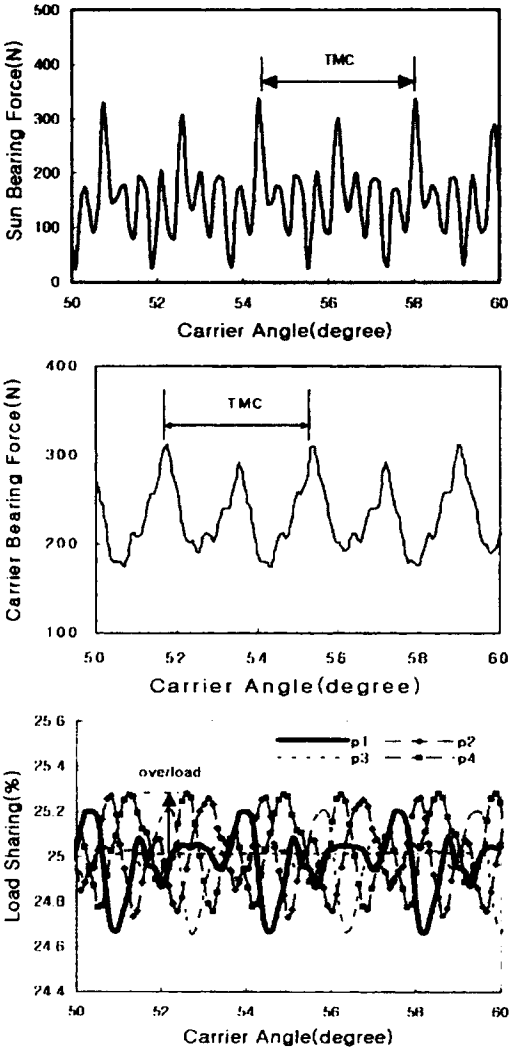

Fig. 3 Bearing forces and planet load sharing under normal conditions with four planets

at a steady state solution after a very short transient period. Only steady state parameters were used for the analysis.

The sun and carrier bearing forces as well as the planet load sharing under normal conditions (no errors) for the four planet case are shown in Fig. 3. Because of the symmetry of the planetary gears, the sun and carrier bearing forces were much smaller than the planet bearing forces. The four planets had different phases because of their unequal spacing. Nevertheless, the four bearings shared the load almost equally, at about 25% each, and overload sharing was small. The bearing forces fluctuated, corresponding to the engagement of each tooth mesh. The acronym TMC indicates one tooth mesh cycle.

Figure 4 shows the planet bearing forces under normal conditions with three planets. The forces of all of the planets were exactly the same due to the equal spacing and the in-phase meshes. Any variation resulted from changes in the number of teeth in contact at each mesh. The sun and carrier bearing forces were always zero.

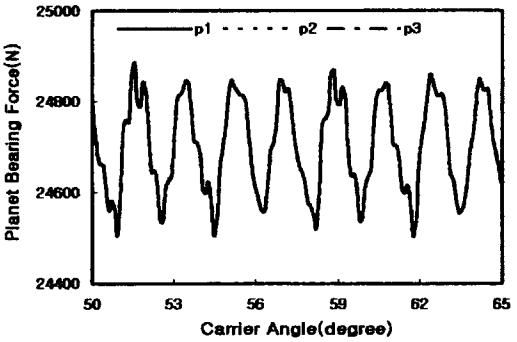

Fig. 4 Planet bearing forces under normal conditions with three planets

3.2 Effects of position error

The resultant sun and carrier bearing forces as well as the planet load sharing with a sun position error with four planets are shown in Fig. 5. The mean and peak-to-peak values of the bearing forces were much higher than with no errors. In addition to fluctuations due to differences in

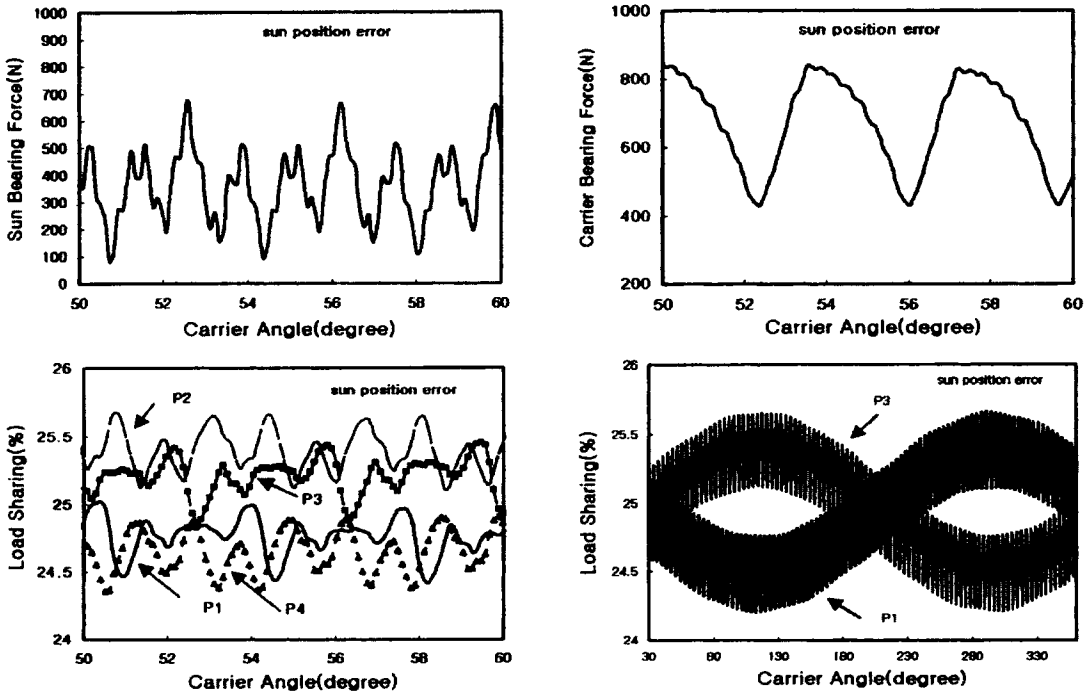

Fig. 5 Sun and carrier bearing forces and planet load sharing with a sun position error of 25 μm with four planets

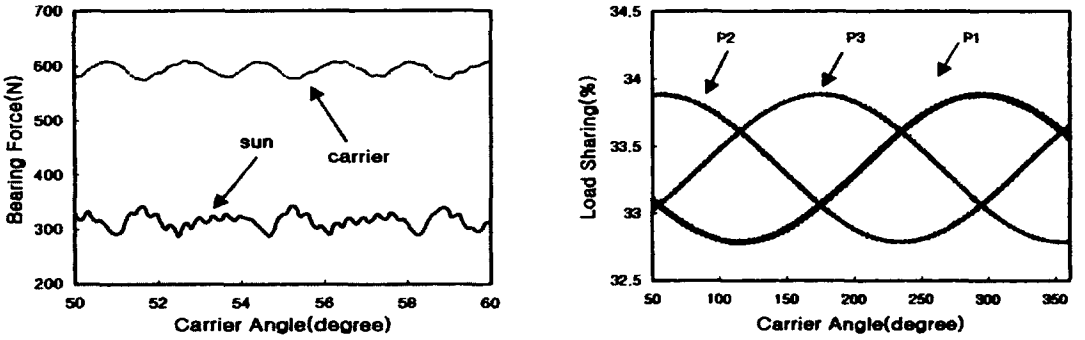

Fig. 6 Sun and carrier bearing forces and planet load sharing with a sun position error of 25 μm with three planets

tooth mesh, the planet bearing forces varied as the planets rotated around the sun. All planet bearing forces and the load sharing had the same mean and peak-to-peak values.

With three planets, the fluctuation in the bearing forces was less than in the four planet case. Nevertheless, the general trends were similar (Fig. 6).

The trends for ring gear position error were qualitatively the same as those for sun gear position error, because the kinematic effects of the two errors are similar.

When the position of the planet pin or the bearing moved an amount from the ideal position toward radial direction (radial position error), all of the results were similar to those obtained under normal conditions, except that the carrier bearing force was slightly higher. Whereas all of the center distances between gears changed when there were sun or ring position errors, only one sun-planet center distance changed due to a planet radial position error.

The bearing forces and planet load sharing with a planet tangential position error (in circumferential direction) are shown in Figs. 7 and 8 for four and three planets, respectively. Because the planet with tangential position error ($p1$) is pushed ahead of the other planets, the bearing of the planet with the error always had the highest load.

Figs. 9 and 10 show the relative trends in the maximum bearing force, overload sharing, and critical stresses due to position error in the four and three planet cases, respectively. The bearing

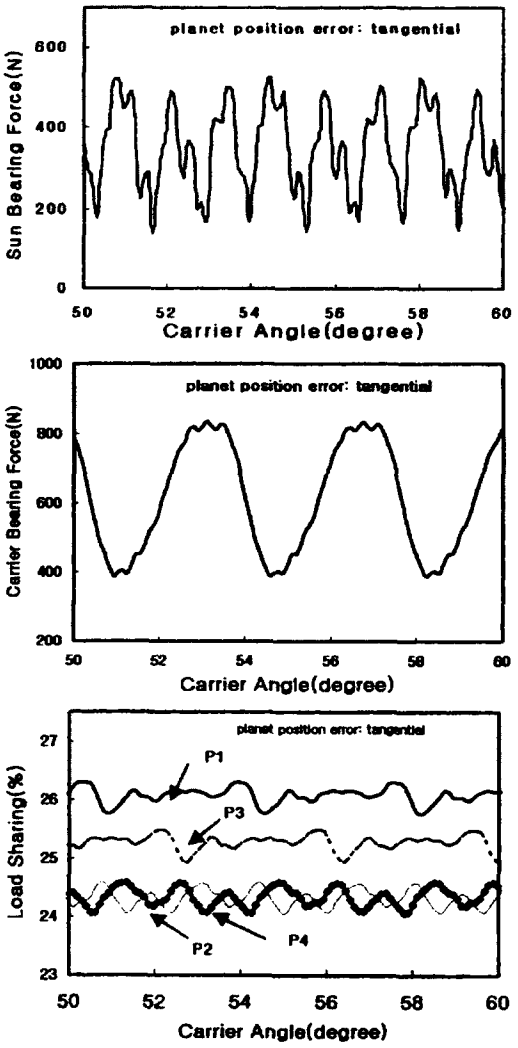

Fig. 7 Sun and carrier bearing forces and planet load sharing with a planet tangential position error of 25 μm with four planets

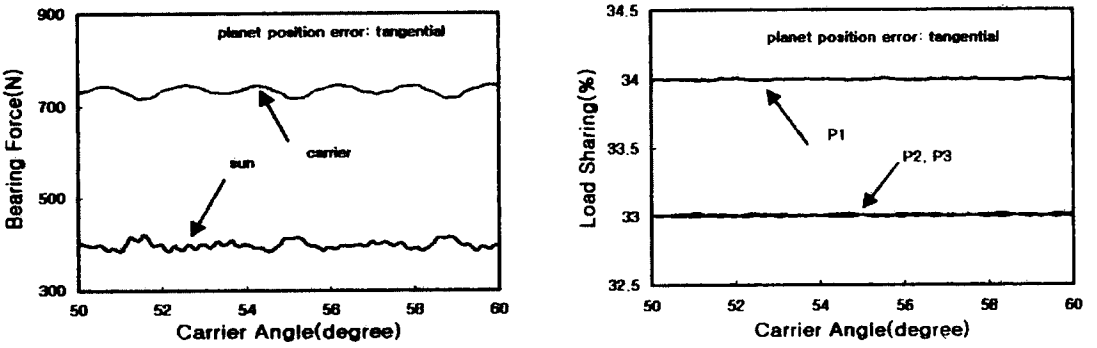

Fig. 8 Sun and carrier bearing forces and planet load sharing with a planet tangential position error of 25 μm with three planets

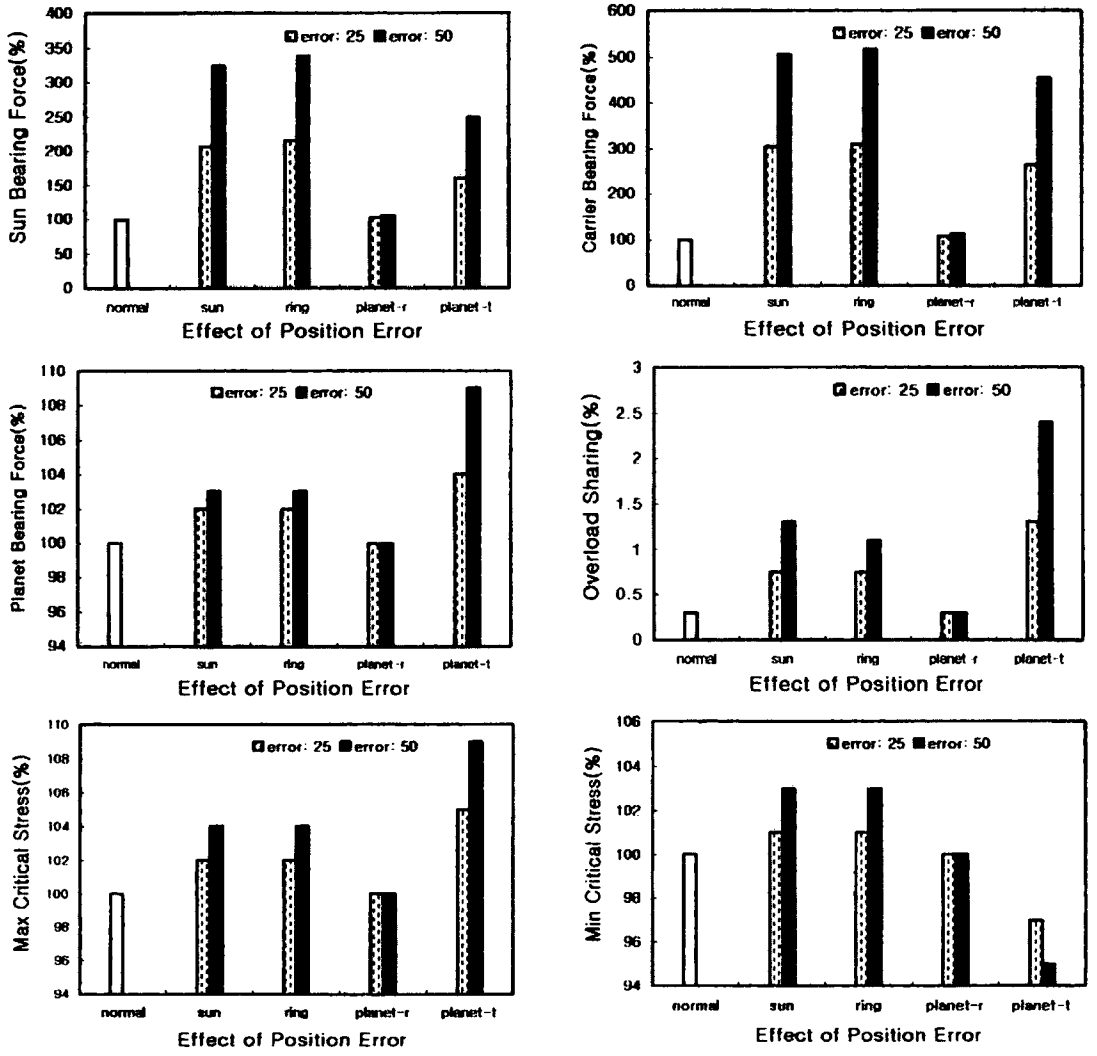

Fig. 9 Trends in the maximum bearing forces and critical stresses due to the effects of a position error with four planets

forces and critical stresses for the four planet case were normalized relative to the values obtained under normal conditions. Because the sun and carrier bearing forces of the three planet case under normal conditions were always zero, these bearing forces were normalized using the values obtained for sun gear errors.

Position errors with four planets, except those due to a planet radial error, induced a rapid increase in the sun and carrier bearing forces, and that increase was proportional to the size of the error. The sun and carrier bearing forces were affected most by sun and carrier errors ; the planet bearing forces were affected most by planet tangential error. Overload sharing was affected most by planet tangential position error. In the four planet case, a planet tangential error caused the greatest increase in the maximum critical stress, but the minimum critical stress for this case decreased to below the values obtained under normal conditions.

The effects of position errors were more dominant for four planet case (different mesh phasing) than for three planet case (same mesh phasing).

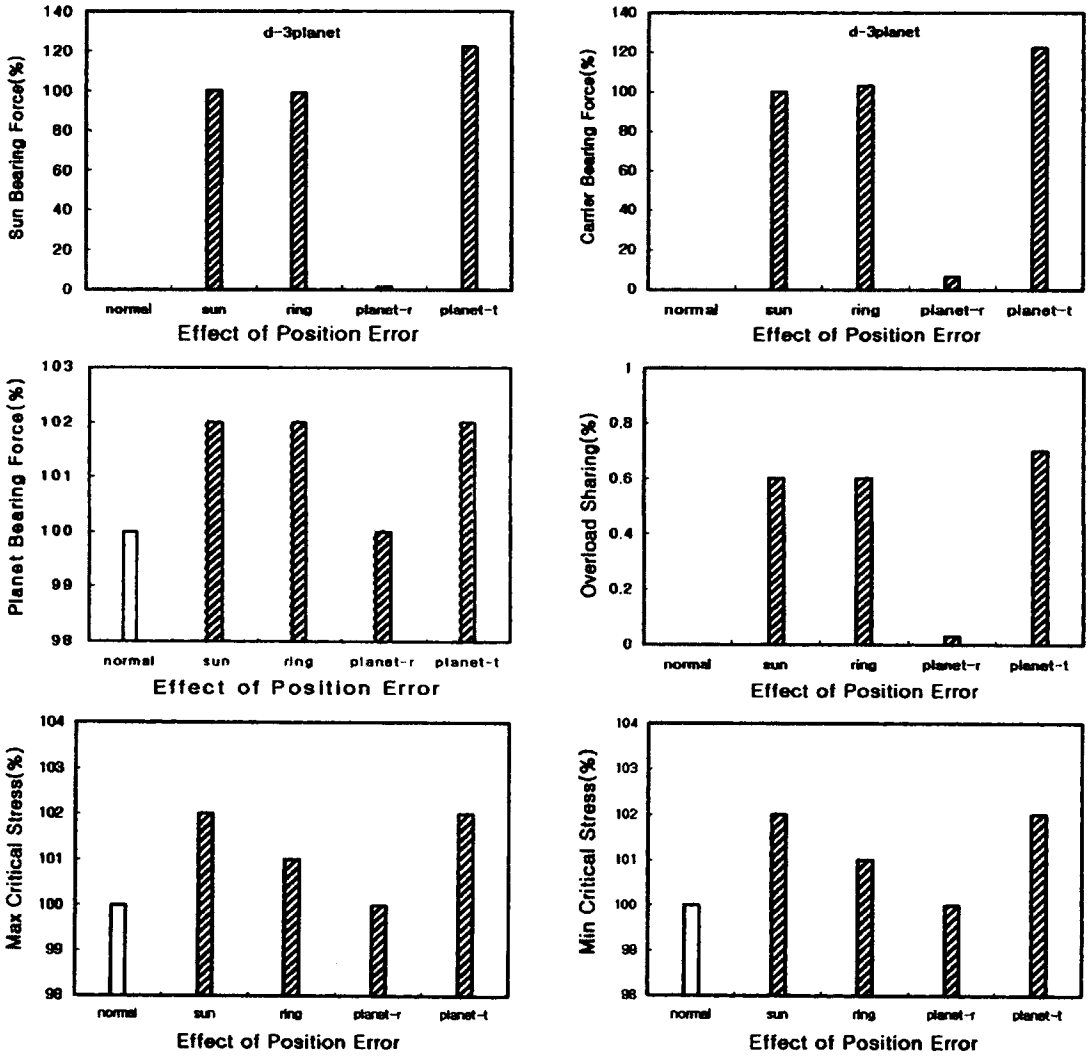

Fig. 10 Trends in the maximum bearing forces and critical stresses due to the effects of a position error with three planets, error=25 μm

3.3 Effects of runout error

The bearing forces and load sharing in the case of sun gear runout error are shown in Fig. 11. The bearing forces were much higher than those obtained under normal conditions. The planet bearing forces had the same peak and mean values, but showed different phasing and additional fluctuations corresponding to the carrier rotation. Except for the fluctuations due to the carrier rotation, the magnitudes and shapes of the bearing forces were similar to those obtained in the case of sun position error. The general trends for the three planet case were similar to those obtained for four planets.

Except for the fluctuations due to the carrier rotation, which consisted of one cycle during one carrier rotation, the magnitudes and patterns of the bearing forces and the load sharing in the case of ring gear runout error were almost the same as those for sun gear runout error.

The sun and carrier bearing forces as well as the planet load sharing in the case of planet

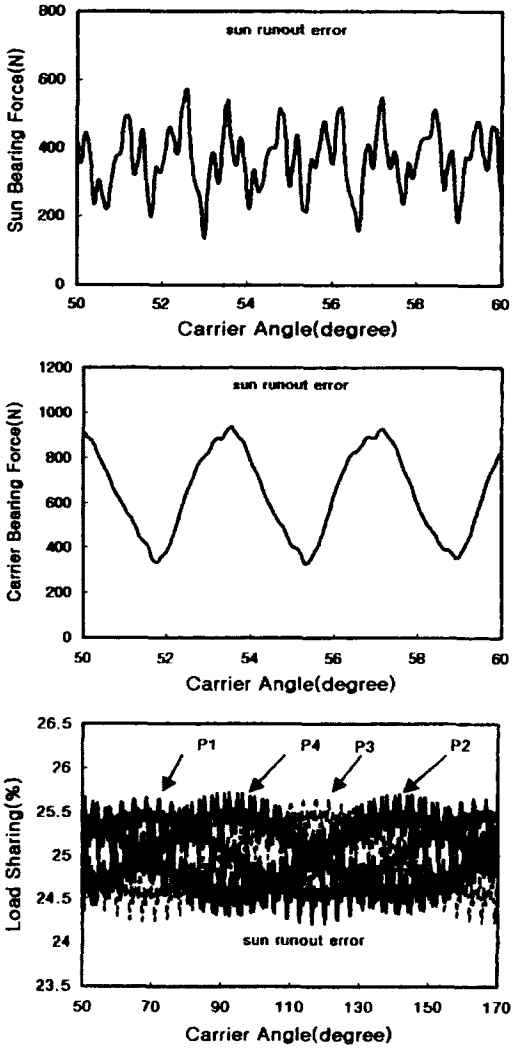

Fig. 11 Sun and carrier bearing forces and planet load sharing with a sun gear runout error of 25 μm with four planets

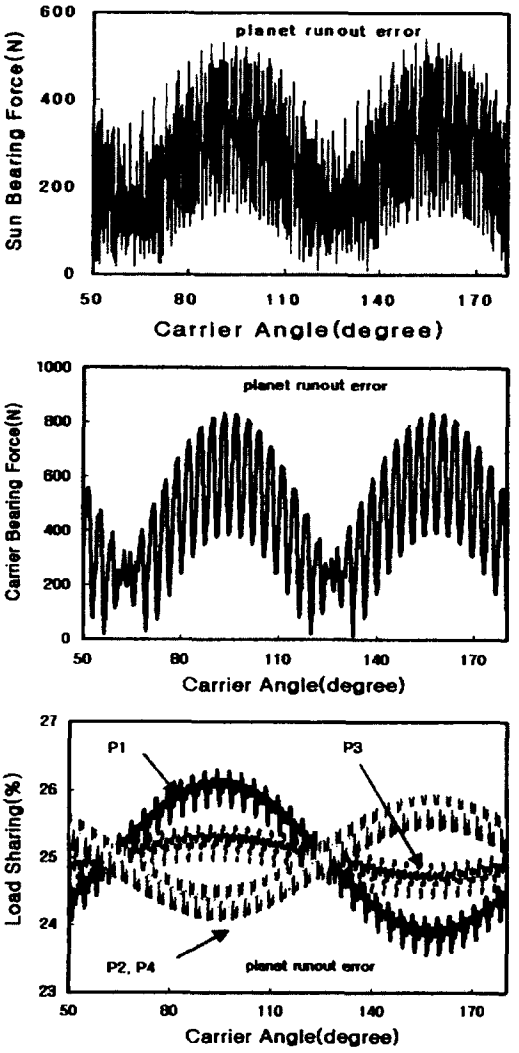

Fig. 12 Sun and carrier bearing force and planet load sharing with a planet runout error of 25 μm with four planets

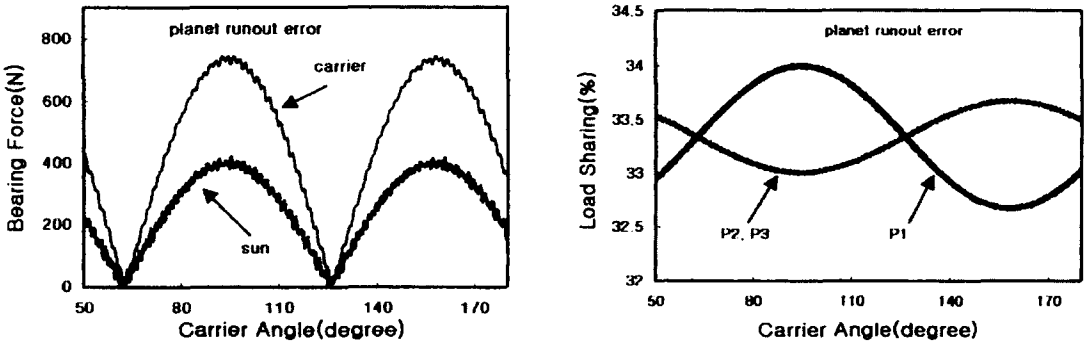

Fig. 13 Sun and carrier bearing force and planet load sharing with a planet runout error of 25 μm with three planets

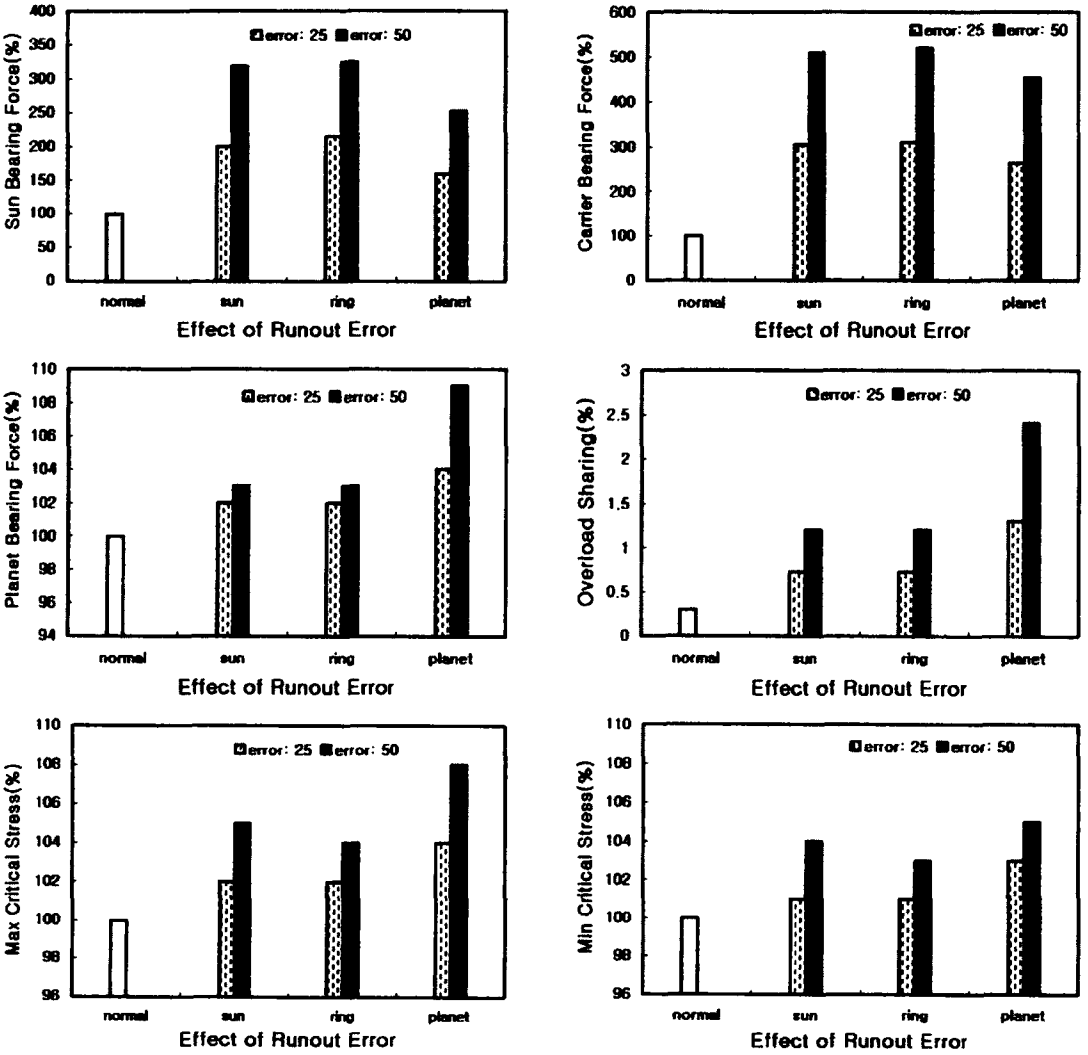

Fig. 14 Trends in the maximum bearing forces and critical stresses due to the effect of runout error with four planets

runout are shown in Figs. 12 and 13 for the four planet and three planet cases, respectively. The sun and carrier bearing forces decreased to zero by symmetry at the moment when all of the planets carried the same load. This caused the peak-to-peak values of the sun and carrier bearing forces to become much larger than under other conditions. The planet bearing forces had the same mean values but different peak-to-peak values. When four planets were used, the symmetric planets had the same phases ($p1$ and $p3$, $p2$ and $p4$). When three planets were used, the planets without errors ($p2$ and $p3$) had the same phases. The planet with the error ($p1$) had the largest peak value in both the four and three planet cases.

Figures 14 and 15 show the relative trends of runout error effects for the four planet and three planet cases, respectively.

Runout errors induced a rapid increase in the sun and carrier bearing forces, and that increase was proportional to the size of the error. Even though the sun and carrier bearing forces under normal conditions with three planets were always

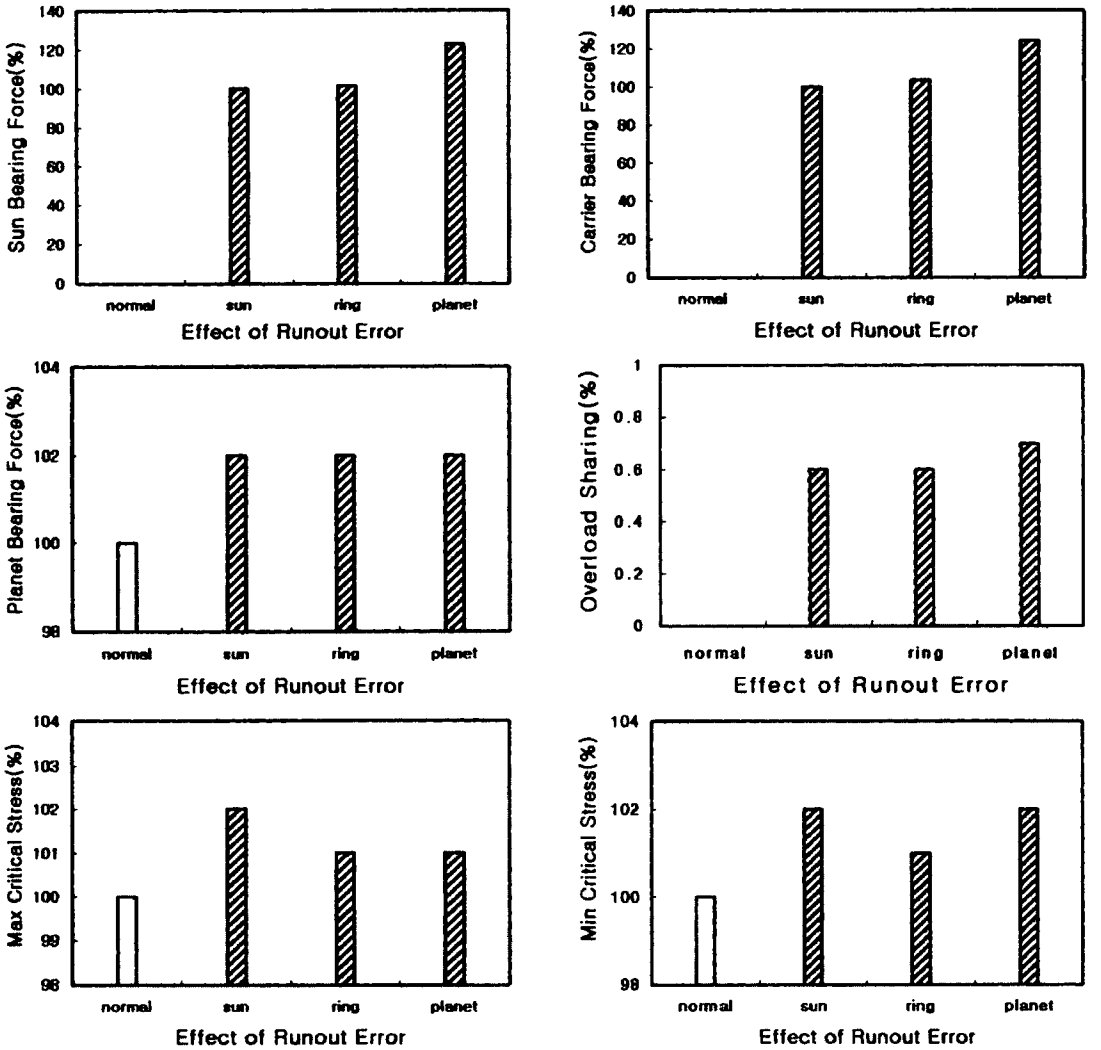

Fig. 15 Trends in the maximum bearing forces and critical stresses due to the effect of runout error with three planets, error=25 μm

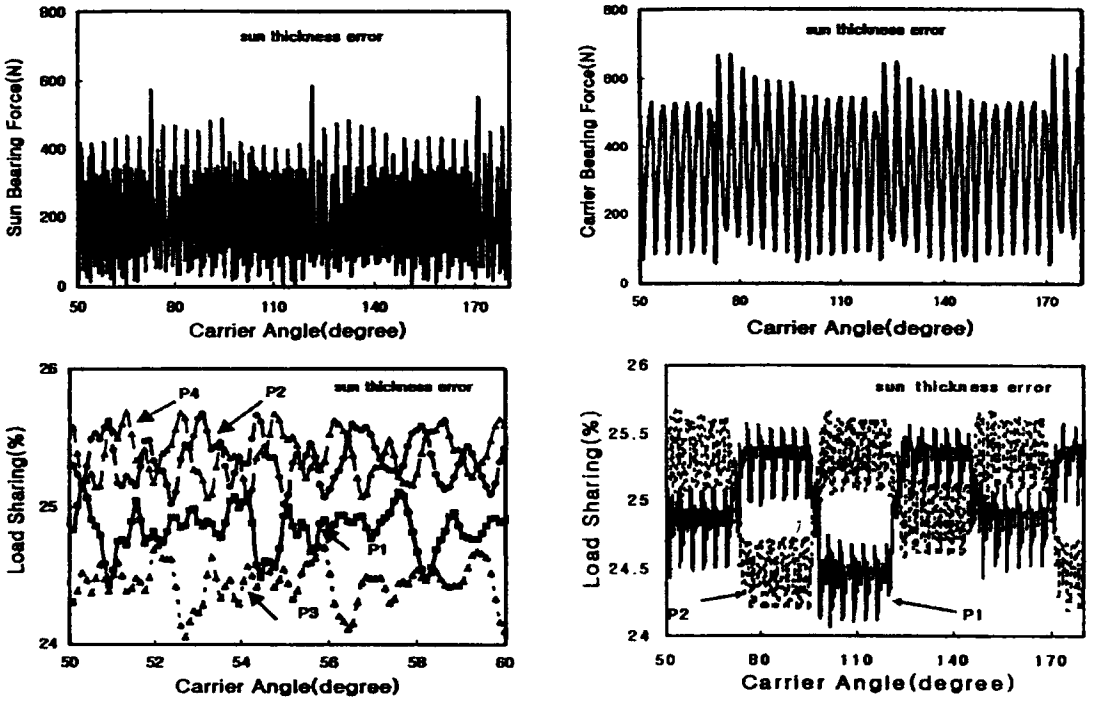

Fig. 16 Sun and carrier bearing forces and planet load sharing with a sun thickness error of 25 μm with four planets

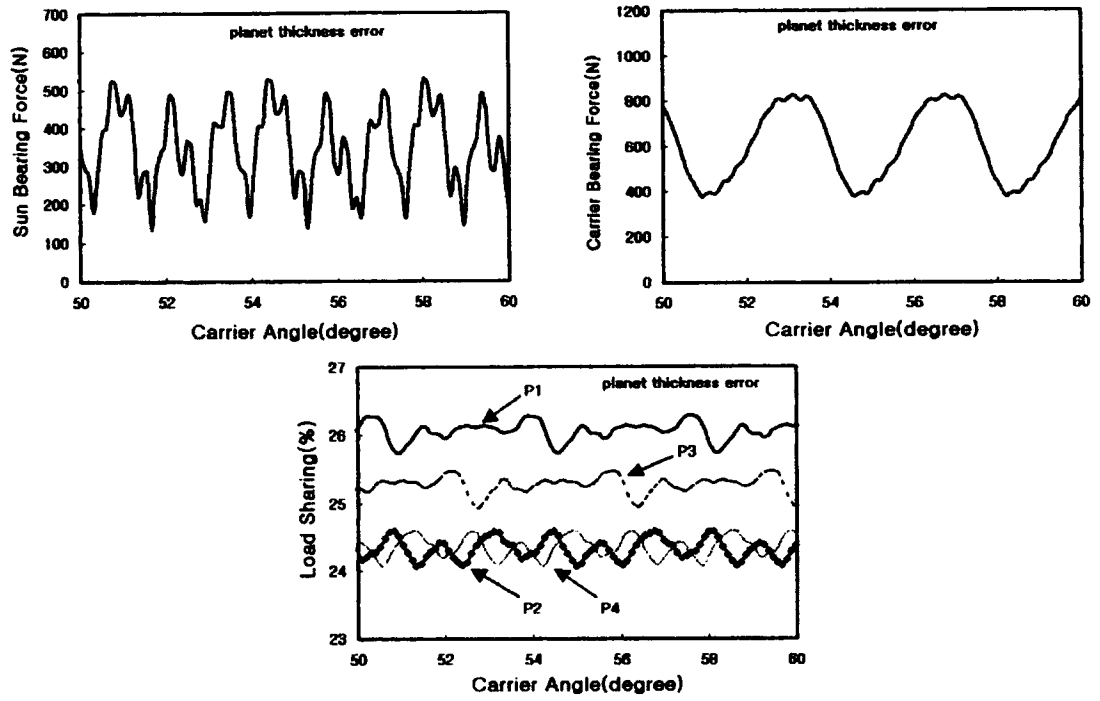

Fig. 17 Sun and carrier bearing forces and planet load sharing with a planet thickness error of 50 μm with four planets

zero, they rapidly increased if there was a runout error in any of the gear elements.

Each bearing force was most affected by each bearing related runout error in the four planet case. However, the effects of planet runout error were always greater for the three planet case.

3.4 Effects of thickness error

Figure 16 shows the bearing forces and load sharing with an error in sun thickness. The bearing forces were greater than those obtained under normal conditions but less than those obtained with position and runout errors. Whenever the part of the sun gear teeth with error began to mesh with new planets, the sun and carrier bearing forces increased rapidly. This trend was more dominant for thickness error than for position and runout errors. The four planet bearings had almost the same mean and peak values, and the planets at symmetric positions had the same phases. When a planet meshed with the part of the sun that had a thickness error, it had the maximum amount of load sharing. Because of the positive thickness error, the affected teeth approached their nominal position earlier than other planets, causing that planet's load to be

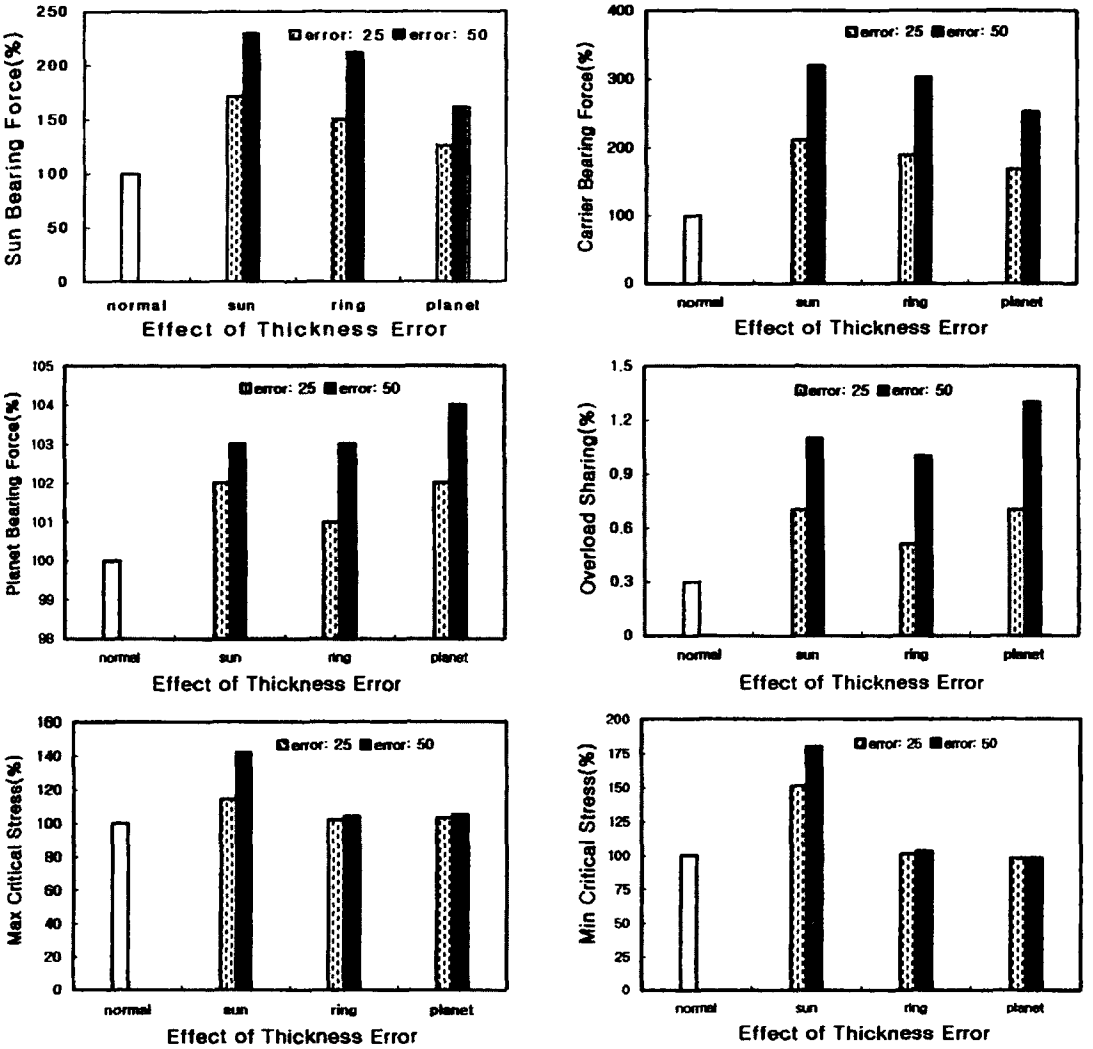

Fig. 18 Maximum bearing forces and critical stresses caused by tooth thickness error with four planets

larger than that of the other planets.

When three planets were used, the three planet bearings had almost the same mean and peak values, and all of the planets had different phases.

The trends of the bearing forces for a ring gear thickness error were almost the same as those for a sun gear thickness error.

For the four planet case, the sun and carrier bearing forces as well as the planet load sharing with an error in planet thickness are shown in Fig. 17.

The bearing forces were greater than those obtained under normal conditions but less than those obtained with position and runout errors. Because the planet with thickness error ($p1$) is pushed ahead of the other planets, the bearing of the planet with the error always had the highest load. And the diagonally opposed planet $p3$ had the second highest value. Since the total of the bearing forces is constant, the bearing forces of $p2$ and $p4$ were the lowest, and had the same mean and peak values.

For the three planet case, $p2$ and $p3$ had the same mean and peak values, as well as the same phases.

Figures 18 and 19 show the relative trends of

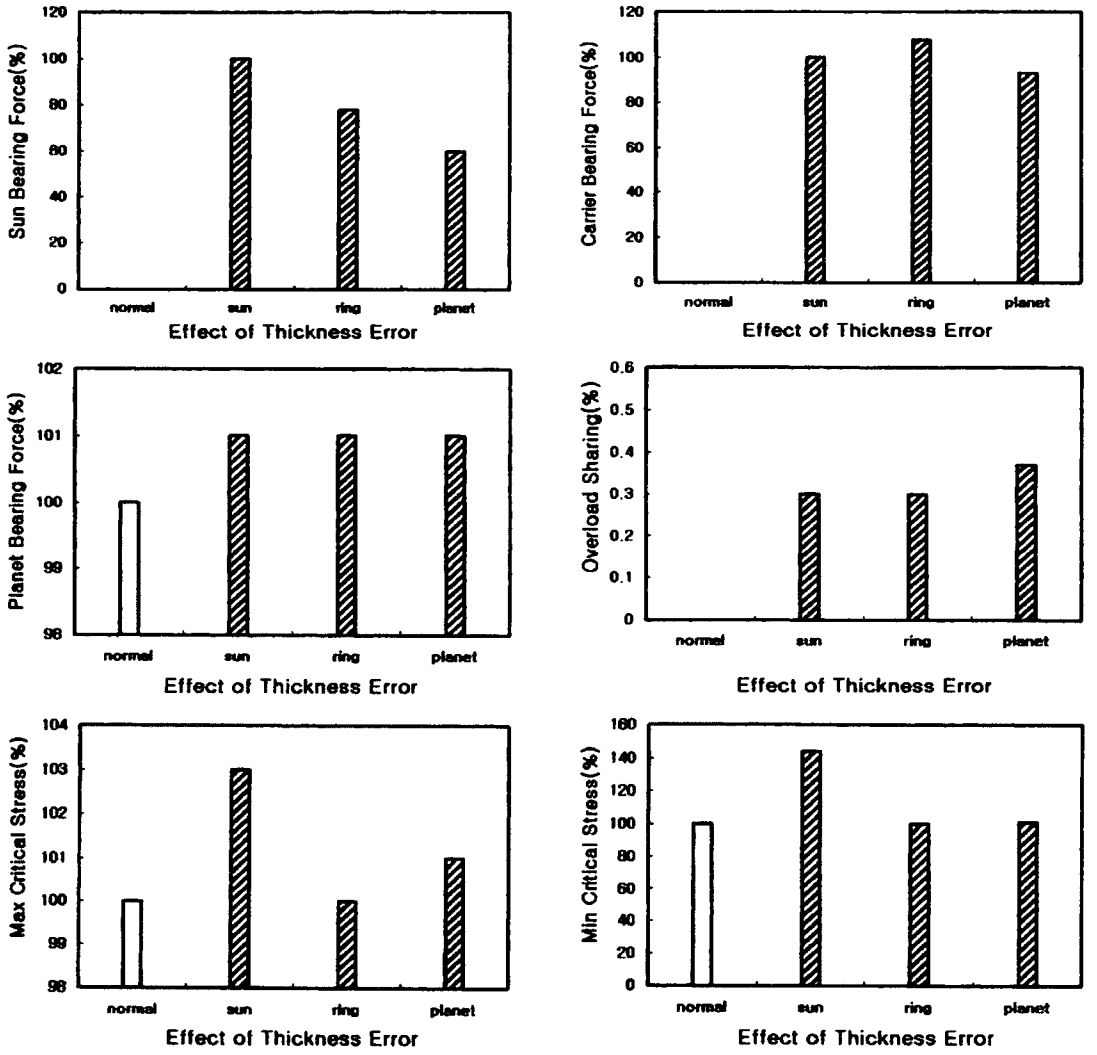

Fig. 19 Maximum bearing forces and critical stresses caused by a 25-μm tooth thickness error with three planets

thickness error effects. The bearing forces were most affected by an error in each related bearing. Except the magnitudes, no specific differences in the general trends for thickness errors were observed between the three planet and four planet cases.

4. Summary and Conclusions

A dynamic analysis was performed using a nominal kinematic analysis combined with a hybrid FE method to characterize the effects of various manufacturing errors on the bearing forces and critical stresses of a planetary gear system.

Bearing forces were little affected by thickness errors as compared to position or runout errors. Each bearing force was most affected by errors in the gear supported by its own bearing. Equal load sharing by the planets was hindered most by planet related errors.

The effects of errors were more dominant for different mesh phasing system than for same mesh phasing system.

The magnitudes of the planet bearing forces were much greater than those of the sun and carrier bearings, and the planet bearing forces and load sharing were the most sensitive to errors in the planet gear. Hence, planet tangential positions and runout errors should be carefully controlled to avoid any problems induced by bearing forces or critical stresses. Planet radial position error had little effect on the dynamic properties of the system.

Although sun and carrier bearing forces are relatively small as compared to planet bearing forces under ideal conditions, manufacturing errors can increase those bearing forces several fold.

Acknowledgment

This paper was supported by Wonkwang University in 2002. We also acknowledge Dr. S. Vijayakar of Advanced Numerical Solutions, Inc. for his guidance and for making available the gear analysis program Planetary2D.

References

ANSol, 2003, "Planetary2D User's Manual," Advanced Numerical Solutions.

Bodas, A. and Kahraman, A, 2001, "Influence of Carrier and Gear Manufacturing Errors on the Static Planet Load Sharing Behavior of Planetary Gear Sets," *Proc. JSME Int. Conf. on Motion and Power Transmissions*, MPT2001-Fukuoka, pp. 633~638.

Cheon, G. J., Lee, D. H., Ryu, H. T., Kim, J. H. and Han, D. C., 1999, "A Study on the Dynamic Characteristics of an Epicyclic Gear Train with Journal Bearing," *SAE 1999-01-1052*.

James, B. and Harris, O., 2002, "Predicting Unequal Planetary Load Sharing Due to Manufacturing Errors and System Deflections, With Validation Against Test Data," *SAE 2002-01-0699*.

Kahraman, A., 1994, "Planetary Gear Train Dynamics," *ASME J. of Mechanical Design*, Vol. 116, pp. 713~720.

Kahraman, A. and Vijayakar, S., 2001, "Effect of Internal Gear Flexibility on the Quasi-Static Behavior of a Planetary Gear Set," *ASME J. of Mechanical Design*, Vol. 123, pp. 408~415.

Kahraman, A., Kharazi, A. A. and Umrani, M., 2003, "A Deformable Body Dynamic Analysis of Planetary Gears with Thin Rims," *J. of Sound and Vibration*, 262, pp. 752~768.

Lin, J. and Parker, R. G., 1999, "Analytical Characterization of the Unique Properties of Planetary Gear Free Vibration," *ASME J. of Vibration and Acoustics*, Vol. 121, pp. 316~321.

Parker, R. G., Agashe, V. and Vijayakar, S. M., 2000a, "Dynamic Response of a Planetary Gear System Using a Finite Element/Contact Mechanics Model," *ASME J. of Mechanical Design*, Vol. 122, pp. 304~310.

Parker, R. G., Vijayakar, S. M. and Imajo, T., 2000b, "Non-Linear Dynamic Response of a Spur Gear Pair: Modelling and Experimental Comparisons," *J. of Sound and Vibration*, 237 (3), pp. 435~455.

Townsend, D. P., 1991, "Dudley's Gear Handbook," McGraw Hill.

Vijayakar, S., 1991, "A Combined Surface Integral and Finite Element Solution for a Three-Dimensional Contact Problem," *Int. J. of Numerical Methods Eng.*, Vol. 31, pp. 525~545.

Youn In-Sung and Cheon Gill-Jeong, 2003, "Dynamic Characteristics of an Epicyclic Gear Train Considering Coriolis Effects," *Transactions of the KSME, A*, Vol. 27, No. 4, pp. 491~498.